Food Chemistry 452 (2024) 139550

Contents lists available at ScienceDirect

Food Chemistry

journal homepage: www.elsevier.com/locate/foodchem

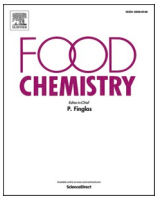

Green fractionation and hydrolysis of fish meal to improve their techno-functional properties

Pedro Barea, Rodrigo Melgosa *, Óscar Benito-Román, Alba Esther Illera, Sagrario Beltrán, María Teresa Sanz

Department of Biotechnology and Food Science (Chemical Engineering Division), University of Burgos, Plaza Misael Bañuelos s/n, 09001 Burgos, Spain

ARTICLE INFO

Keywords:
Fish meal protein
Water fractionation
Hydrolysis
Subcritical water
Emulsification

ABSTRACT

A green strategy employing water as solvent has been adopted to obtain protein hydrolysates from fish meal (FM), its water-soluble fraction (WSP), and its non-water-soluble fraction (NSP). The techno-functional properties of the hydrolysates have been investigated and compared to hydrolysates obtained with Alcalase®. In general, SWH hydrolysates presented higher content of free amino acids and higher degree of hydrolysis, which reflected on the molecular size distribution. However, Alcalase® hydrolysates presented better solubility (from 74 ± 4% for NSP at pH = 2 up to 99 ± 1% for WSP at pH = 4–7). According to fluorescence experiments, FM and NSP hydrolysates showed the highest surface hydrophobicity, which has been related to better emulsifying properties and higher emulsion stability. The emulsions stabilized with 2%wt. of SWH-treated NSP showed the smallest particle sizes, with D[4,3] = 155 nm at day 0, and good stability, with D[4,3] = 220 nm at day 7, proving that water fractionation followed by SWH treatment is a good method to improve the techno-functional properties of the hydrolysates.

1. Introduction

Fish meal is the main co-product of the fish industry, together with fish oil. Fish meal production has increased over the last years, reaching >16 million tonnes in 2020 (FAO, 2022), mainly linked to its utilization in aquaculture and as an ingredient in the pet-food industry. Fish meal presents a high protein content as well as a valuable lipid fraction composition. However, the rise of novel sources of protein resulting from the increasing demand of a growing and aging population urge fish meal producers to explore new processing methods and obtain valuable novel products. Increasing processing yield and efficiency in the utilization of these resources may further reduce the environmental footprint of food produced from marine resources. Therefore, optimal utilization of fish co-products as part of the biomass, which is unavoidably harvested, and development of technologies enabling their value addition to high quality proteins is urgently needed.

Fish co-products contain valuable proteins, polyunsaturated fatty acids (PUFAs), essential amino acids, vitamins, and minerals (Wisuthiphaet & Kongruang, 2015; H. Wu, Forghani, Abdollahi, & Undeland, 2022). Moreover, fish-derived protein hydrolysates have been reported to have remarkable bioactive effects, such as antioxidant, anticancer, antimicrobial, antihypertensive, immunomodulatory, and antithrombotic activities, among others (Shahidi, Varatharajan, Peng, & Senadheera, 2019). Techno-functional properties of fish protein hydrolysates have also been reported, including good solubility, foaming, gelling, and emulsifying properties. These functional properties are closely related to the physicochemical characteristics of the proteins, peptides, and amino acids, such as molecular weight, amino acid composition and surface hydrophobicity (Chen et al., 2019), and play a very important role in the texture and sensory quality of food during processing and storage (Brishti et al., 2020; N. Li et al., 2022).

Subcritical water hydrolysis (SWH) of proteins has been proposed as an environmentally friendly alternative to exploit the valuable compounds present in fish co-products. Subcritical water treatment uses liquid water at temperatures between 100 and 374 °C. At these conditions, the dielectric constant decreases as temperature rises due to hydrogen bond dissociation, making water an effective solvent for moderately polar to non-polar substances. Moreover, the ionic product of water (K_W) increases significantly with temperature, enhancing the concentrations of hydronium and hydroxide ions. This enables water to

* Corresponding author.
E-mail addresses: pbgomez@ubu.es (P. Barea), rmgomez@ubu.es (R. Melgosa), obenito@ubu.es (Ó. Benito-Román), aeillera@ubu.es (A.E. Illera), beltran@ubu.es (S. Beltrán), tersanz@ubu.es (M.T. Sanz).

https://doi.org/10.1016/j.foodchem.2024.139550
Received 16 October 2023; Received in revised form 18 April 2024; Accepted 1 May 2024
Available online 7 May 2024

function as an acid or base catalyst, facilitating the hydrolysis of biomass from different origins, such as lignocellulosic polymers and proteins, into smaller oligomers and peptides without requiring additional catalysts (Ali et al., 2023; Melgosa et al., 2021). For these reasons, SWH can be considered greener than the widely employed chemical and enzymatic methods, providing a purer final extract without need of reprocessing. Previous works have already reported important benefits of SWH compared to enzymatic hydrolysis, such as the higher degree of hydrolysis and release of amino groups that can be achieved in a similar reaction time and with no need of additional catalysts or reagents (Barea et al., 2023). Moreover, increasing temperature and acidifying the reaction media with pressurized CO_2 enhanced the hydrolysis process and the free amino acid release, which have been also associated to better physicochemical and bioactive properties of the FPHs, such as higher antioxidant capacity (Barea et al., 2023). However, few studies have explored the influence of the preparation method on important techno-functional properties of fish meal hydrolysates, such as solubility, surface hydrophobicity, and emulsifying capacity. These properties may be influenced by environmental factors and processing conditions and make the fish protein hydrolysates much more interesting in a wide variety of fields, highlighting food, cosmetic and pharmacy industry. The different fractionation and hydrolysis processes conducted on a protein sample determine the molecular structure of the hydrolysates and their further capacity as a techno-functional ingredient (Lv, Chen, Liu, Xu, & Zhong, 2023).

In this work, the double role of the greenest solvent, water, is emphasized. First, water has been used as a solvent for the fractionation of fish meal proteins. On the other hand, water in subcritical conditions has been used as hydrolytic agent, avoiding the use of chemical solvents and strong acids and alkalis in the production of fish protein hydrolysates. The products obtained from the hydrolysis of the different substrates: fish meal (FM), and the water-soluble protein (WSP) and non-water-soluble protein (NSP) fractions, will be characterised in terms of protein content and amino acid composition. Besides, the different techno-functional properties of the hydrolysates obtained by using only water as solvent and hydrolytic agent will be evaluated. The results obtained can be further used to enhance the use of fish protein hydrolysates in different applications (e.g.: feed and food, cosmetics, or pharmaceutical products), enhancing the sensory, nutritional, and physicochemical properties, while simultaneously improving the economy of its production.

2. Experimental

2.1. Materials

Fish meal from tuna (*Thunnus* sp) was kindly supplied by Sarval Bio-Industries Noroeste, S.A.U. (A Coruña, Spain). It was provided in a powdered formulation and used as it is. Characterization has been carried out in a previous work (Barea et al., 2023), finding a moisture content of 3.4 ± 0.1% (*w*/w); the crude protein, ash, and lipids, expressed in a dry basis, were 51 ± 2%, 21.7 ± 0.2%, and 6.5 ± 0.2% (w/w), respectively. Until use, the fish meal was stored in sealed air-tight polypropylene bags under refrigeration conditions (4 °C) and protected from light.

2.2. Fractionation of fish meal

Fish meal fractionation was achieved by water extraction. Based on previous studies (Barea et al., 2023), fish meal was mixed with water at a ratio of 16 g fish meal/100 mL water (16:100) in a stirred reactor thermostated at 80 °C for 30 min. Subsequently, the resulting slurry was cooled down and filtered through a cheese cloth to obtain a liquid fraction, the water-soluble protein (WSP), and a solid fraction, the non-water-soluble protein (NSP), which was gently dried in an oven at 40 °C for 48 h.

Further characterization analysis and hydrolysis experiments were performed with the original fish meal (FM) and the WSP and NSP fractions, which were stored at −18 °C prior to analysis.

2.3. Subcritical water hydrolysis (SWH)

Subcritical water hydrolysis (SWH) of FM, and WSP, and NSP fractions was performed in a lab-built discontinuous reactor with an internal volume of 0.5 L. The equipment has been described elsewhere (Barea et al., 2023).

For the solid samples, 20 g of FM or NSP were charged into the reactor and suspended in 200 mL of distilled water. In the case of the liquid WSP fraction, SWH process was carried out in a similar way, except that 200 mL of the filtered liquid were directly charged into the reactor and no additional water was used. In a typical experiment and based on previous studies (Barea et al., 2023), hydrolysis temperature was set at 180 °C and pressure at 50 bar. Pressurization of the reactor was achieved using CO_2, which causes acidification of the reaction medium and promotes efficient protein hydrolysis (Barea et al., 2023). After 300 min of SWH process, the vessel was cooled down and depressurized when the temperature was lower than 90 °C. Subsequently, the hydrolysates were withdrawn, filtered through Whatman no. 5 filter paper to separate the solids in the case of the FM and NSP extracts, and frozen at −18 °C for further analysis.

2.4. Enzymatic hydrolysis

Based on previous studies (Barea et al., 2023), the commercial protease Alcalase®, kindly donated by Novo Nordisk A/S, was selected in this work. The protease activity was already determined in a previous work (Barea et al., 2023) by the casein method, resulting in 1157 ± 74 μmol of tyrosine/mL of enzyme preparation.

In the enzymatic hydrolysis study, 10 g of solid (FM, or NSP) were charged into a jacketed glass reactor and suspended into 100 mL of phosphate buffer at pH 8. When the temperature reached 60 °C, the reaction was started by adding 225 U of pre-warmed Alcalase®. In the case of WSP, 100 mL of the liquid obtained in the fractionation step were filtered and charged into the reactor, which was preheated at 60 °C, and mixed with 225 U of preconditioned Alcalase®. Enzymatic hydrolysis was carried out for 24 h at constant temperature of 60 °C. After that, the mixture was immersed in boiling water for 5 min to inactivate the enzyme and subsequently cooled down in an ice bath, filtered through Whatman no. 5 filter paper and frozen at −18 °C for further analysis.

2.5. Freeze drying

Freeze-dried protein hydrolysates (FDH) were obtained from the liquid and filtered hydrolysates produced in the SWH process and in the enzymatic hydrolysis. First, liquid hydrolysates were placed in a Petri dish and equilibrated at −80 °C for 2 h. Then, the frozen samples were submitted to freeze-drying at $1.5{\cdot}10^{-4}$ mbar (Telstar Lyoquest) until moisture was lower than 3%wt.

After lyophilization, the FDHs were weighed in order to calculate the final hydrolysis yield. FDHs were stored in dark hermetic flasks under refrigeration conditions (4 °C) for further analysis.

2.6. Characterization

Samples from the FM, WSP and NSP substrates and their corresponding FDHs were analyzed in order to evaluate the fractionation and hydrolysis process.

2.6.1. Elemental analysis

The elemental composition (C, H, N, S) of the original FM, WSP and NSP fractions and the FDHs was determined by elemental microanalysis in an EA Flash 2000 apparatus (Thermo Scientific, USA), equipped with

a thermal conductivity detector (TCD). Oven temperature was set at 900 °C and gas flows were 250 mL/min for oxygen and 140 mL/min for helium, used as the carrier gas. A second flow of helium (100 mL/min) was used as a reference for the detector, whereas the calibration curve was prepared with different concentrations of 4-Aminobenzenesulfonamide.

2.6.2. Amino acid profile

The amino acid profile was analyzed by gas chromatography (Hewlett-Packard, 6890 series) with an EZ:faast AAA GC kit, following the method described by (Trigueros et al., 2021). Amino acid profile of FM, WSP and NSP substrates was determined after hydrolysis using 6 N HCl at 100 °C during 24 h and further derivatization. Since tryptophan and cysteine are lost by acid hydrolysis, and methionine can be partially destroyed, an alkaline hydrolysis was also carried out to determine these amino acids (Trigueros et al., 2021). Arginine cannot be detected by this kit and asparagine and glutamine were quantified as aspartic and glutamic acids, respectively.

Free amino acids in the FM, WSP and NSP substrates were determined by derivatization and GC-FID analysis, following the previously described method (Trigueros et al., 2021) without prior HCl or alkaline hydrolysis. The difference between total amino acids after hydrolysis and free amino acids were referred to as bound amino acids. Free amino acids were also determined for the FDHs.

2.6.3. Degree of hydrolysis

The degree of hydrolysis (DH) was estimated by the ninhydrin reaction method according to the Sigma Aldrich protocol. 1 mL of ninhydrin reagent solution was gently mixed with 2 mL of sample and heated for 10 min at 100 °C using a boiling water bath. Afterwards, the samples were cooled, and 5 mL of 95% ethanol were added. The absorbance was measured at 570 nm. A calibration curve was constructed using a leucine solution daily prepared (Friedman, 2004). The DH was evaluated according to the equation by (Adler-Nissen, 1979):

$$\mathrm{DH}\ (\%) = \frac{h}{h_{tot}} \times 100 \quad (1)$$

where h is the number of equivalent peptide bonds hydrolyzed, expressed as meq/g protein and h_{tot} is the total amount of millimoles of individual amino acids per gram in the unhydrolyzed protein that can be evaluated from the amino acid profile.

2.7. Physicochemical and techno-functional properties of the hydrolysates

2.7.1. Protein solubility (PS)

PS was determined according to the method described by (N. Li et al., 2022) with some modifications. In brief, 10 mg of lyophilized extracts were dispersed in 20 mL of distilled water maintained at different pH values (pH 2.0, 4.0, 7.0 and 10.0) by adding HCl or NaOH. The mixture was stirred for 15 min and then centrifuged at 8000*g* for 30 min. The nitrogen content of the supernatants was measured using the Lowry method as described by (Barea et al., 2023). PS was expressed as percentage ratio of the protein content of the supernatant to the total protein content. Results are expressed as the mean of three replicates.

2.7.2. Surface tension

Surface tension was measured in an optical tensiometer (Attension Theta, Biolin Scientific), using the pendant drop method. Briefly, 2 g of FDH were dispersed in 95 mL of distilled water at ambient temperature. Droplets of ca. 4 μL were created with the help of a microsyringe, which was fixed to the apparatus and aligned to a high-resolution camera. Images of the pendant drop were taken during 10 s to measure the drop volume and radius, and the surface tension was calculated from these measurements using the OneAttension software (Biolin Scientific). Results are reported as the average of three measurements.

2.7.3. Molecular weight distribution of the hydrolysates

The molecular size distribution of the FDHs was measured by Gel Permeation-Size Exclusion Chromatography (GPC-SEC) in an HPLC system (Agilent 1260 infinity II) coupled to a refraction index detector (RID). The column system consisted of a Proteema precolumn (4.6 × 30 mm) and a micro column (4.6 × 250 mm) with a porosity of 100 Å and a particle size of 3 μm (PSS Polymer Standards Service GmbH), which allowed for good separation in the range from 150 to 100,000 Da. The mobile phase was 0.01 M ammonium acetate at a flow rate of 0.3 mL/min. Separation and detection were conducted at 35 °C. Data acquisition and GPC-SEC calculations were performed using OpenLab CDS 3.2 and its GPC-SEC add-on. For calibration, a standard set of pullulans (PSS Polymer Standards Service GmbH) was used. Both standards and FDH samples were dissolved in ultrapure water at a concentration of 10 g/L. After filtration through 0.45 μm syringe filters, a volume of 10 μL was injected.

2.7.4. Protein fluorescence

2.7.4.1. Intrinsic fluorescence. Intrinsic fluorescence analysis was performed as described by (Arogundade, Mu, & Akinhanmi, 2016) with slight modifications. FDHs were dissolved in phosphate buffer solution (pH = 6.8–7.0) at a concentration of 0.5 mg/mL. Intrinsic fluorescence emission spectra were obtained by a fluorescence spectrophotometer (Cary Eclipse, Agilent Technologies). Sample solutions were excited at 280 nm, and emission spectra were recorded from 300 nm to 800 nm. Slit width was set at 5 nm, both for excitation and emission, in order to minimize the effect of tyrosine residues.

2.7.4.2. Quenching experiments. Fluorescence quenching experiments were also performed by adding different concentrations of potassium iodide (KI) to the FDH solutions, based on the method developed by (Benito-Román et al., 2019). Maximum fluorescence data of each sample against a blank with no added KI was recorded in order to obtain the Stern-Volmer plots and calculate the quenching constant (K_{SV}) according to the following equation:

$$\frac{I_0}{I} = 1 + K_{SV}[Q] \quad (2)$$

where $[Q]$ is the concentration of quencher (KI).

Results are reported as the means of three replicates. Blank samples with no added KI were diluted with the same volume of phosphate buffer in order to account for the dilution effect.

2.7.5. Emulsifying properties

2.7.5.1. Preparation of emulsions. Oil-in-water (O/W) emulsions were prepared using FDHs as emulsifying agents. Emulsions were prepared as follows: First, 2 g of FDH were dispersed in 95 mL of distilled water. Then, 3 g of sunflower oil were added dropwise and continuously stirring. This coarse emulsion was subsequently homogenized in a Miccra D-9 homogenizer-disperser for 3 min at 21.000 rpm. The resulting pre-emulsion was immediately passed through a microfluidizer (Microfluidcs LM20) equipped with an F20Y interaction chamber. Final microemulsions were obtained at a fixed pressure of 150 MPa and 7 passes through the microfluidizer. A cooling coil immersed in ice water was used to keep the emulsion at controlled temperature throughout the homogenization process. Each emulsion was duplicated to account for experimental error.

For each FDH, droplet size distribution was measured after each pass in the microfluidizer. The stability of the final microemulsions was assessed by droplet size measurements over 14 days of storage under refrigeration conditions (4 °C).

2.7.5.2. Determination of the droplet size distribution and stability of the emulsions. The droplet size of the emulsions was measured by static light scattering (SLS) using a Mastersizer 2000 (Malvern Instruments) immediately after emulsification. Emulsion droplet size values are reported as the volume-weighted mean diameter (De Brouckere mean diameter; D[4,3]) and as droplet size distributions from 20 nm to 2000 μm. Results are reported as the mean of three measurements.

2.7.5.3. Electrokinetic potential of emulsions. The electrokinetic potential (i.e. ζ potential) of emulsion droplets stabilized with FDHs was measured by electrophoretic mobility using a Zetasizer Nano Series equipment (Malvern Instruments, UK). ζ potential measurements were conducted after dilution of emulsions in ultrapure water (1:20). Then, with the help of a gel-loading tip, samples were added to the bottom of a disposable capillary cell specifically designed for this measurement (O'Sullivan, Beevers, Park, Greenwood, & Norton, 2015). Results are reported as the average and standard deviation of ten replicates, with 50 stabilization cycles per replicate.

3. Results and discussion

3.1. Fractionation of fish meal protein according to water solubility

According to previous studies (Barea et al., 2023), the initial protein content of FM is 51 ± 2% (*w*/w), as determined by the analysis of elemental N and the corresponding conversion factor, which was calculated from the amino acid profile (Table S1). Water fractionation yielded a liquid extract containing around 4% (*w*/*v*) soluble solids and 20.5 ± 0.8 mg protein/mL, according to the Lowry assay (Barea et al., 2023), which represents half of the soluble solids and one third of the total protein content in the fish meal. The other two thirds of protein in FM plus other non-soluble components4 formed the NSP fraction, with an estimated protein content of 50% (w/w) according to the mass balance.

The amino acid profile of FM and its fractions, WSP and NSP, is reported in Table S1. From these data and according to the NREL standard protocols (Sluiter, Ruiz, Scarlata, Sluiter, & Templeton, 2010), the nitrogen-to-protein conversion factors (NPCFs) were calculated. For the FM, and the WSP and NSP fractions, NPCFs of 4.98, 4.59, and 4.91 were obtained, respectively. Similar NPCF values have been reported in the literature for fish and derivatives (Boisen, Bech-Andersen, & Eggum, 1987; Diniz, Barbarino, Oiano-Neto, Pacheco, & Lourenço, 2013; Salo-Väänänen & Koivistoinen, 1996), indicating a higher-than-average proportion of N in the fish meal proteins (around 20% wt.). With these factors and the elemental analysis of N (results not shown), the crude protein content of the samples was estimated to be 51.3, 54.4, and 54.7 g protein/100 g for FM, WSP and NSP, respectively, finding good agreement with the mass balance calculations.

Despite the similarities in the NPCFs of the FM and its fractions, some differences in the amino acid profiles can be observed. As indicated in Table S1, the percentage of large non-polar amino acids (ILE, LEU, MET, PHE, TRP) is higher in the NSP fraction, followed by the original FM and lastly the WSP fraction. On the contrary, the content of small amino acids such as ALA, GLY, PRO and CYS is greater in the WSP fraction compared to the NSP, indicating some selectivity of the fractionation process with water at 80 °C. As we describe in the following sections, the different amino acid profiles of FM, WSP and NSP substrates further affect the extension of the hydrolysis process and especially the properties of the final hydrolysates.

3.2. Hydrolysis of fish meal and its fractions

FM, WSP and NSP were subjected to SWH and enzymatic hydrolysis. Liquid hydrolysates were freeze-dried to obtain the FDHs. Chemical characterization of the FDHs was carried out in terms of free amino acid release to the medium. As shown in Table S1, production of free amino acids during the hydrolysis process was most pronounced when the WSP fraction was used as the starting material, and almost 5 times higher with the SWH method, compared to the enzymatic hydrolysis with Alcalase®. Among the free amino acids released, the proportion of large non-polar amino acids follows the same trend as in the non-hydrolyzed samples, being higher in the NSP hydrolysate compared to FM and WSP. Moreover, the WSP hydrolysates showed a lower ratio than the original WSP, indicating low hydrolysis of the non-polar domains and the potential transformation of these large non-polar amino acids into smaller amino acids and degradation products, following different reaction pathways (Abdelmoez, Nakahasi, & Yoshida, 2007). In the literature, several authors have demonstrated that SWH is a suitable method to produce free amino acids from fish and shellfish by-products. For instance, semi-continuous SWH of sardine viscera produced a free amino acid yield of 161.2 mg/g dry hydrolysate at 140 °C (Melgosa et al., 2020), whereas Chun et al. (Chun et al., 2022) reported free amino acid yields of 65.3–74.8 mg/g dry extract for the SWH of comb pen shell viscera in a batch reactor at 170–230 °C during 15 min. The incorporation of CO_2 to the SWH process.

In the literature, the optimal SWH temperature and time to obtain free amino acids vary greatly (Marcet, Álvarez, Paredes, & Díaz, 2016). Higher temperatures generally lead to higher amino acid productions, as shown by (Park, Roy, Kim, Lee, & Chun, 2022) in the extraction of amino acids from eel by-products. In that work, an eel extract containing 6.7 g/L of free amino acids was obtained by using SWH in a discontinuous reactor at 220 °C for 15 min (Park et al., 2022). However, higher temperatures and longer exposure times lead to decreased yields due to thermal degradation into organic acids (Marcet et al., 2016).

Elemental (CHNS) analysis of the FDHs obtained in this work is reported in Table 1. These data allowed the calculation of the elemental H/C and N/C ratios, which range between 1.85 and 1.96 and 0.24–0.30, respectively, for all the hydrolysates. O/C values are missing due to limitations in the analytical procedure. Despite these limitations, we can

Table 1
Elemental composition, hydrolysis yield, and degree of hydrolysis of the freeze-dried hydrolysates (FDHs) obtained from fish meal (FM), its water-soluble fraction (WSP), and its non-water-soluble fraction (NSP) by subcritical water hydrolysis (SWH) and enzymatic hydrolysis with Alcalase® (Alc).

	C (%)	H (%)	N (%)	S (%)	Protein (%wt.) *	Hydrolysis yield (g FDH/100 g)	Degree of hydrolysis (DH, %) †
				SWH			
FM	44.9 ± 0.3	7.4 ± 0.3	13.5 ± 0.2	n. d.	67.5 ± 1	31.9 ± 0.5	72 ± 2
WSP	34.1 ± 0.4	5.4 ± 0.1	11.9 ± 0.1	n. d.	54.6 ± 0.5	99.8 ± 0.2	86.5 ± 0.5
NSP	50.6 ± 0.1	7.8 ± 0.1	14.7 ± 0.1	n. d.	72.2 ± 0.6	28.5 ± 0.5	52 ± 1
				Alc			
FM	34.2 ± 0.6	5.6 ± 0.1	10.7 ± 0.1	n. d.	53.5 ± 0.5	26.3 ± 0.5	23.6 ± 0.2
WSP	28.1 ± 0.7	4.6 ± 0.2	9.6 ± 0.2	n. d.	44 ± 1	98.9 ± 0.7	33.8 ± 0.5
NSP	30.2 ± 0.7	4.8 ± 0.1	11.3 ± 0.1	n. d.	55.7 ± 0.2	19.7 ± 0.3	9.4 ± 0.3

* Nitrogen to Protein Conversion Factor, NPCF = 4.98 for FM, 4.59 for WSP, and 4.91 for NSP.

† DH (%) $= \frac{h}{h_{tot}} \times 100$ (Adler-Nissen, 1979).

see that these values fall very well within the Multidimensional Stoichiometric Compound Classification Constraints (MSCCC) proposed by (Rivas-Ubach et al., 2018) for protein compounds. The crude protein content of the hydrolysates can be also calculated by using the NPCFs previously calculated for FM, WSP and NSP. Except for the WSP fraction hydrolyzed with Alcalase®, the hydrolysates presented similar or slightly more crude protein than their non-hydrolyzed counterparts. This is especially true for the SWH-treated FM and NSP hydrolysates, with around 70% of these FDHs being of protein nature. It seems clear that the enhanced protein content has been achieved through selective hydrolysis of proteins and solubilization of peptides and amino acids, as shown in the results for the hydrolysis yield. For WSP, hydrolysis yield, expressed as the amount of FDH obtained from 100 g of solid material, was close to 100% in all cases since all the solids were already solubilized; therefore, no selectivity could be achieved, and the protein content was similar to that of the non-hydrolyzed NSP. On the other hand, FM and NSP fraction showed hydrolysis yields ranging from 20 to 35%. As expected, the hydrolysis of FM presented higher yield than that of NSP due to the presence of soluble solids, whereas all the solids in the NSP fraction were initially not soluble. In any case, these rather low hydrolysis yields came with the benefit of a higher protein selectivity.

Together with the hydrolysis yield, the degree of hydrolysis (DH) is an indicative of the extension of the hydrolysis process. DH values are reported in Table 1 as the percentage of cleaved bonds over the total

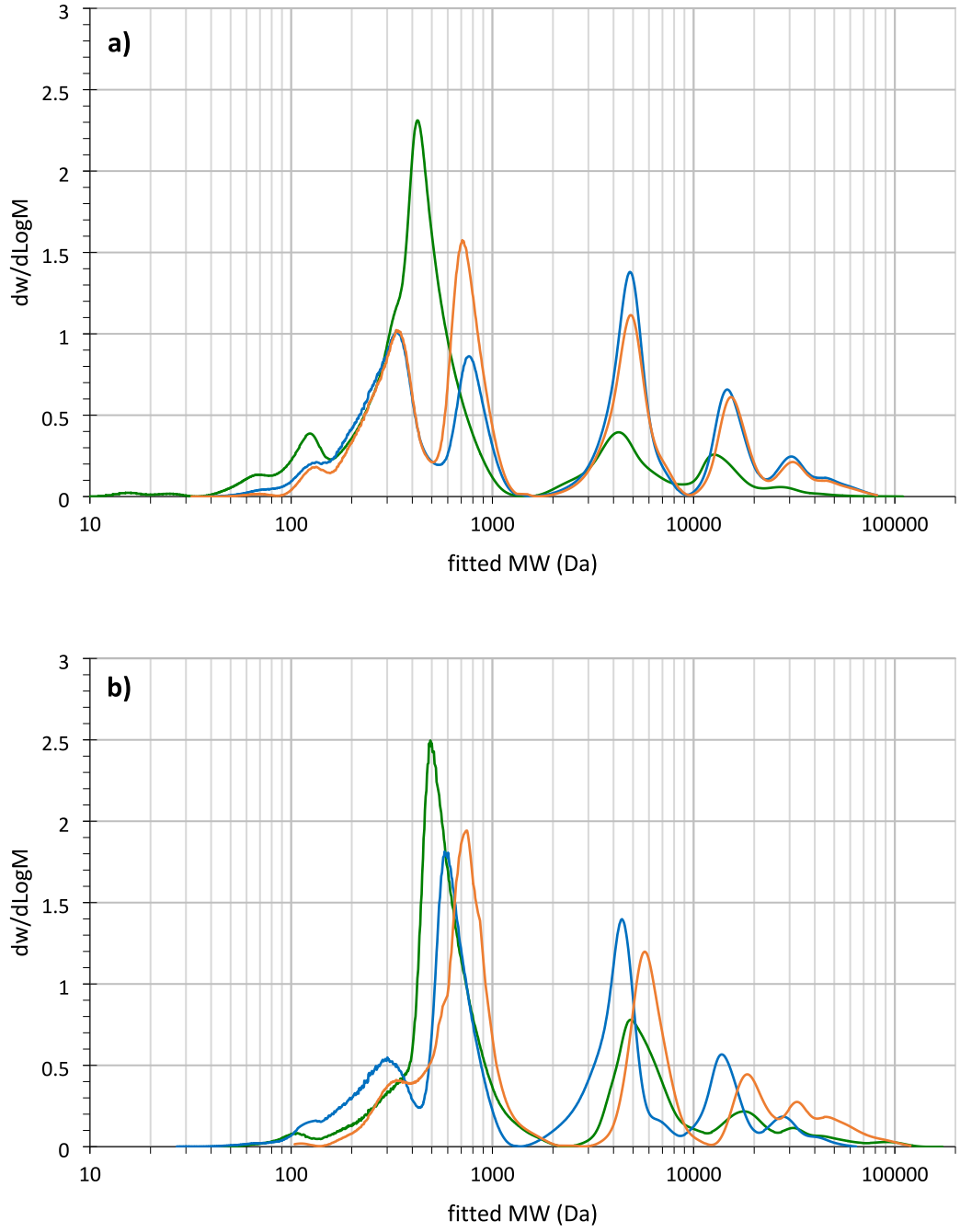

Fig. 1. Normalized slice distributions of hydrolysates obtained from fish meal (FM, orange), its water-soluble fraction (WSP, green), and its non-water-soluble fraction (NSP, blue) by a) subcritical water hydrolysis (SWH) and b) enzymatic hydrolysis with Alcalase® (Alc).
Samples were resuspended in ultrapure water at 10 g/L. (For interpretation of the references to colour in this figure legend, the reader is referred to the web version of this article.)

peptide bonds present in the original protein, which can be calculated from the amino acid profile. These results showed that SWH achieved much higher DH compared to enzymatic hydrolysis with Alcalase® regardless of the starting material. Considering both the DH and the crude protein content of the hydrolysates, we can observe similarities with enzymatic hydrolysis as reported by other authors (Aspevik, Egede-Nissen, & Oterhals, 2016), since protein recovery remained constant and even decreased when DH increased. In this work, the different substrates and hydrolysis methods affect the composition and characteristics of the final hydrolysate. This way, Alcalase® hydrolysis provided low protein recovery and DH values. On the contrary, SWH of the same fractions achieved higher DHs, with the lowest protein content and highest DH of all the hydrolysates obtained in this work for WSP fraction. Overall, the SWH process presents higher efficiency in the hydrolysis and solubilization of fish proteins than enzymatic hydrolysis with Alcalase®, since results obtained in this work showed slightly higher selectivity, increased hydrolysis yields and higher DHs.

3.3. Molecular weight distribution of the hydrolysates

Molecular weight distribution of hydrolysates showed complex elution profiles, with similarities between samples that can be attributed to their common origin. Differences in size and abundance can be also observed and might be related to the techno-functional properties of the hydrolysates, as it will be discussed in the following sections. Results obtained are represented in Fig. 1 as a normalized distribution of slice molecular weights against the estimated MW according to column calibration.

Fig. 1a shows large peaks in the range 200–1000 Da, indicating that SWH process promotes the formation of small peptides. While FM and NSP presented 2 groups of compounds with MW centered around 300 and 600 Da, WSP only showed one peak centered at 400 Da that may correspond to di- or tri-peptides as it has been also observed in a previous work (Barea et al., 2023). SWH hydrolysates presented some larger peptides and proteins, with estimated MWs centered at 4 kDa, 11–12 kDa, and 28–30 kDa, which are more abundant in FM and NSP hydrolysates than in WSP, probably due to the abundance of these compounds in the original substrates. On the other side, free amino acids are likely represented in the small peak centered around 100 Da, since their MWs range from 75 Da for glycine ($C_2H_5NO_2$) to 204 Da for tryptophan ($C_{11}H_{12}N_2O_2$). The abundance of these compounds is notable in the SWH hydrolysates, especially in that from WSP, and is much lower in Alcalase® hydrolysates, which is in accordance with the previously described results for the amino acid profile and degree of hydrolysis.

In the case of the hydrolysates obtained with Alcalase® (Fig. 1b), most of the compounds were also in the range 200–1000 Da. Again, WSP only presented one peak at 400 Da whereas FM and NSP presented two groups of compounds at 300 and 600 Da. However, the peak at 300 Da was much smaller than in the SWH hydrolysates, indicating less abundance of small peptides in the Alcalase hydrolysates. In general, the normalized distributions of Alcalase® hydrolysates at MW larger than 1000 Da are rather similar and have as well some resemblances with the SWH hydrolysates. Three main families of compounds can be observed at MW = 4–6, 11–14 and 28–30 kDa. Differences in abundance and displacement of the peaks to lower MW give an idea of the susceptibility of each substrate to enzymatic hydrolysis with SWH and Alcalase®. Area calculations allowed to estimate a weighted-average molecular size for each hydrolysate, being: 4835, 2021 and 5335 Da for FM, WSP and NSP obtained by SWH, respectively; and 6792, 4057 and 4065 Da for FM, WSP and NSP obtained by enzymatic hydrolysis.

3.4. Protein solubility (PS)

Solubility of FDHs in aqueous buffer at different pH is reported in Fig. 2. Comparing the different hydrolysates, the WSP hydrolysates presented the higher solubility, reaching values close to 100% at mild pH conditions (pH = 4.0–7.0) for WSP hydrolyzed with Alcalase®. In the case of WSP hydrolyzed with SWH, total solubility is only achieved at pH = 4.0. Outside of this pH range, solubility of WSP hydrolysates would decrease down to ca. 95%, which is still very high. This is not unexpected since the original protein was obtained by water solubilization at a similar pH, and its further hydrolysis would increase its solubility in a wider range of pH and temperatures due to the smaller size of the obtained protein residues. The explanation may lie in the higher content of polar groups of WSP, compared to the other substrates, which gives

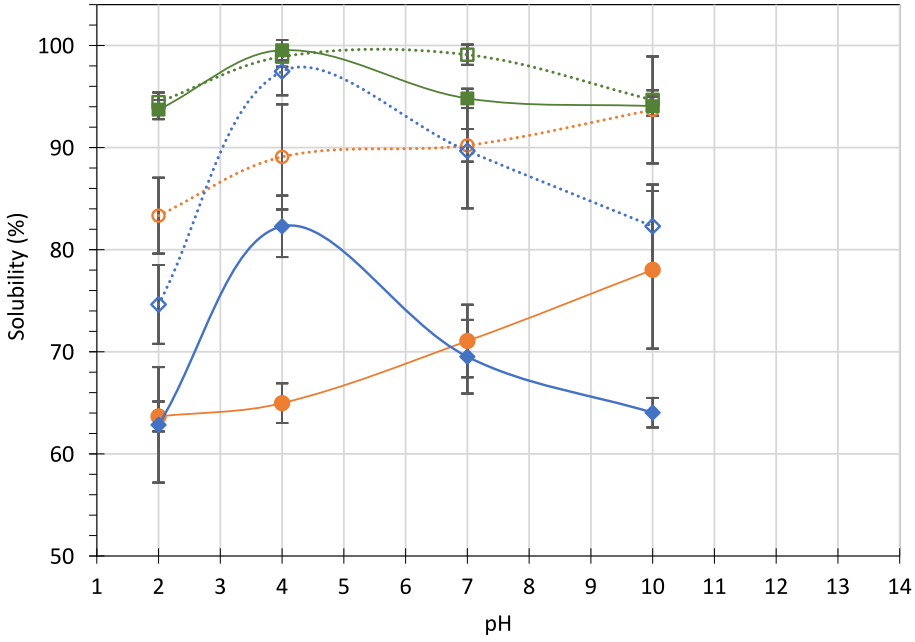

Fig. 2. Effect of pH on the solubility of freeze-dried hydrolysates (FDHs) obtained from fish meal (FM, ● ○), its water-soluble fraction (WSP □ ■), and its non-water-soluble fraction (NSP, ◆ ⋄) by subcritical water hydrolysis (SWH, full symbols) and enzymatic hydrolysis with Alcalase® (Alc, hollow symbols). Samples were resuspended at 500 mg/L in buffer solutions at pH = 2.0–10.0. Lines are drawn to guide the eye.

place to electrostatic interactions between water molecules and protein residues (Gehring, Davenport, & Jaczynski, 2009).

On the contrary, the presence of hydrophobic amino acid residues would promote protein-protein interactions and aggregation into insoluble species (Gehring et al., 2009), leading to lower solubility values as observed for the NSP hydrolysates. In this case, a more significant effect of pH on solubility can be observed, varying in the ranges 82–97% and 64–82% in the FDHs obtained by enzymatic hydrolysis and SWH, respectively. Both Alcalase® and SWH hydrolysates followed the same trend, with the lowest solubility at pH = 2.0, increasing dramatically up to the maximum solubility at pH = 4.0 and then decreasing again at higher pH values. The enzymatic FDHs, despite having a larger molecular size than SWH hydrolysates according to the GPC-SEC results, present significantly higher solubility than their SWH counterparts for all the pHs studied in this work. It has been proposed that Alcalase®, being an endopeptidase, acts by cleaving larger proteins into more soluble polypeptide chains (Barea et al., 2023); whereas SWH mostly liberates small peptides and free amino acids, which are also soluble but affect less the solubility parameter since the parent protein is still large and insoluble. Another possible reason for the lower solubility of SWH hydrolysates might be related to the high temperatures of SWH treatment, which may have promoted the denaturation and unfolding of the polypeptide chains, rendering some of the proteins and peptides insoluble due to the higher exposure of hydrophobic domains (López et al., 2019). For FM hydrolysates, higher solubility was also obtained with Alcalase® compared to SWH in all the pHs studied. We can also observe that solubility increases with pH, from 80% and 60% at pH = 2.0 to 95% and 75% at pH = 10.0, for Alcalase® and SWH, respectively. At high pH, carboxyl groups are charged but not amine groups; thus, repulsive intermolecular interactions between local negatively charged groups may promote protein-water interactions and the observed increase in solubility (Das, Mir, Chandla, & Singh, 2021).

3.5. Surface tension

The potential use of the protein hydrolysates obtained in this work as emulsifiers is based on the modification of interfacial and surface properties of emulsions and solutions. As shown in Fig. 3 and taking ultrapure water as a reference, the surface tension at room temperature (20 °C) notably decreases when the hydrolysates are present. The more drastic decrease was observed for the SWH-treated WSP fraction, whereas the highest surface tension was found in FM subjected to enzymatic hydrolysis.

Results obtained in the measurement of surface tension of the protein hydrolysates show the potential of FDHs as emulsifying and stabilizing agents. Thanks to their molecular structure and amphiphilic nature, small peptides and amino acids can adsorb into the oil-water interphase, decreasing the energy required to form the emulsion and stabilizing the emulsion droplets.

3.6. Intrinsic fluorescence

It has been reported that the intrinsic fluorescence of proteins is primarily due to the presence of tryptophan residues within its structure (Bobone, Van De Weert, & Stella, 2014), among other hydrophobic amino acids such as tyrosine. Denaturation of the protein, protein hydrolysis, and changes in its environment may cause changes in protein folding and the exposure of hydrophobic domains, where tryptophan is more abundant. These changes can be monitored through the determination of the fluorescence emission spectra of the protein (Antonov, Zhuravleva, Cardinaels, & Moldenaers, 2015).

As shown in Fig. 4, enzymatically hydrolysed FDHs had lower emission maximum (λ_{max}) values than those obtained by SWH. These results indicate that the tryptophan residues were mostly embedded into the protein structure, within a hydrophobic environment (C. Li, Xue, Chen, Ding, & Wang, 2014). Based on these results, the enzymatically hydrolysed FDHs would present more hydrophilic domains on the surface of the FDH, promoting interactions with water molecules and possibly explaining their higher solubility at different pH (2−10) when compared to those obtained by SWH.

On the other hand, intrinsic fluorescence of FDHs obtained by SWH presented higher fluorescence intensity than its Alcalase® counterparts

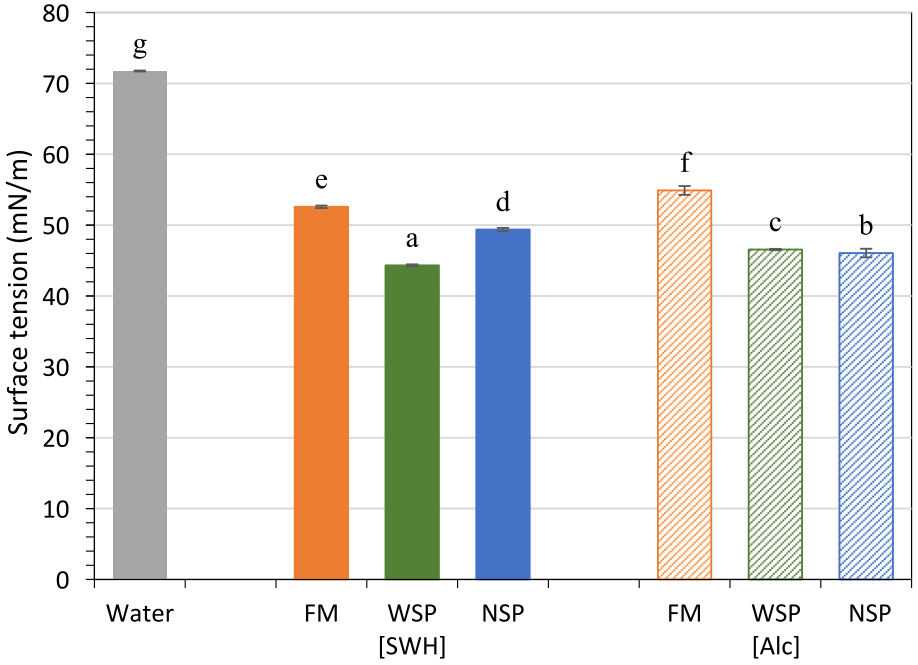

Fig. 3. Surface tension measured at room temperature (20 °C) of freeze-dried hydrolysates obtained from fish meal (FM, orange), its water-soluble fraction (WSP, green), and its non-water-soluble fraction (NSP, blue) by subcritical water hydrolysis (SWH, full columns) and enzymatic hydrolysis with Alcalase® (Alc, patterned columns). All samples consisted of 2 g of solid resuspended in 93 mL of ultrapure water. Different letters represent statistically significant differences at $p < 0.05$. (For interpretation of the references to colour in this figure legend, the reader is referred to the web version of this article.)

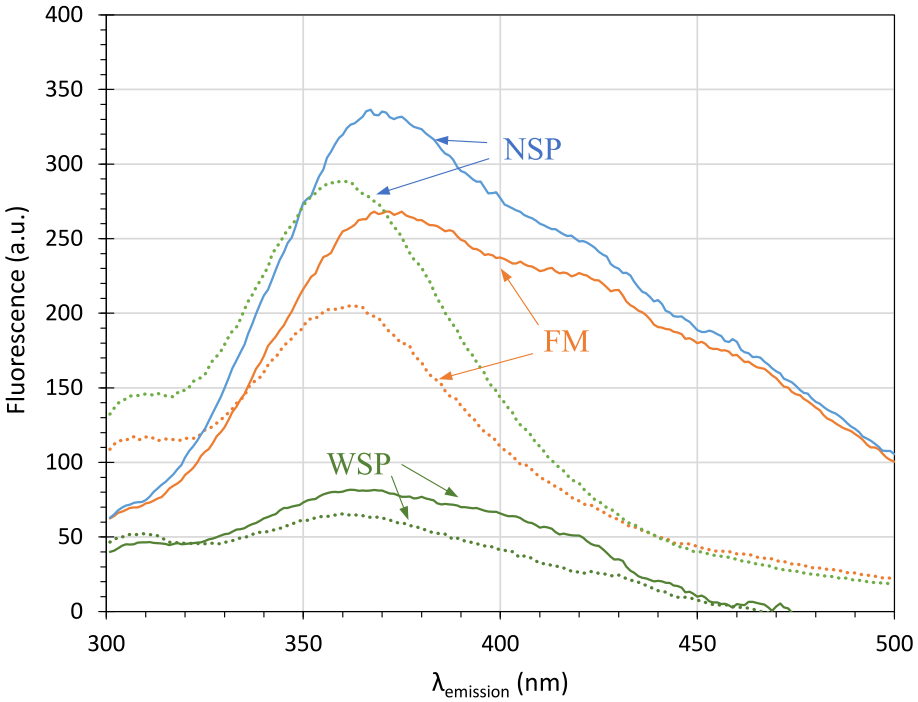

Fig. 4. Intrinsic fluorescence emission spectra of freeze-dried hydrolysates (FDHs) obtained from fish meal (FM, orange), its water-soluble fraction (WSP, green), and its non-water-soluble fraction (NSP, blue) by subcritical water hydrolysis (SWH, continuous lines) and enzymatic hydrolysis with Alcalase® (Alc, dotted lines). Samples were resuspended at 0.5 mg/mL in phosphate buffer at pH = 6.8. (For interpretation of the references to colour in this figure legend, the reader is referred to the web version of this article.)

at the same concentration. Moreover, the fluorescence emission maxima of SWH hydrolysates are red shifted in relation to the enzymatic FDHs, especially for FM and the NSP fraction. This phenomenon may occur when the fluorophores are highly exposed to the solvent and indicates deep changes in the molecular structure of the protein (C. Li et al., 2014), which are likely due to the extensive hydrolysis and unfolding of the proteins by SWH treatment. SWH and enzyme-mediated protein hydrolysis leads to protein unfolding and a gradual transition of the more hydrophobic domains from the core of the protein to the surface, yielding a more flexible protein conformation. Hence, these flexible proteins with higher surface hydrophobicity could have excellent emulsifying properties since they would adsorb to the oil-water interface, decreasing the surface tension and establishing interactions with both hydrophobic and hydrophilic molecules (N. Li et al., 2022).

Comparing by substrates, it is highly noticeable that the hydrolysates obtained from WSP presented the lower fluorescence intensities, followed by those from FM, and NSP with the highest emissions. Since tryptophan and other fluorescent amino acids are hydrophobic, it seems likely that the WSP fraction contains lower quantities of these residues, whereas the NSP fraction presented a higher proportion of this hydrophobic amino acid. Besides, the shoulder centred around 310 nm observed in the spectra of Alcalase®-hydrolyzed samples, and not in the SWH hydrolysates, may be due to the tyrosine residues of the enzyme (Paiva dos Santos, Mellinger-Silva, Santa Brígida, & Barros Gonçalves, 2020).

3.7. Surface hydrophobicity of the FDHs

Fluorescence quenching is an adequate method to determine the presence and exposure to the solvent environment of tryptophan residues within the protein structure; hence, it is a good indicator of the surface hydrophobicity of the protein (N. Li et al., 2022). From the results obtained in the quenching experiments, a Stern-Volmer plot was obtained for each FDHs. The fitting parameters are shown in Table S2, with K_{SV} values ranging from 3.16 ± 0.08 to 12.9 ± 0.2 M^{-1} and intercepts close to 1. In general, SWH hydrolysates showed higher K_{SV} values than their Alcalase® counterparts, indicating a larger number of hydrophobic groups exposed to the solvent environment. It is likely that the higher degree of hydrolysis achieved by this method would have led to protein unfolding and higher extent of exposure of hydrophobic groups in proteins. This is especially true for the FM and NSP hydrolysates. On the other hand, low K_{SV} values have been frequently attributed to partial denaturation and subsequent aggregation of hydrophobic residues (He et al., 2014; Ma et al., 2018), which may be the case for the WSP hydrolysates. However, it is more likely that the lower presence of hydrophobic residues in the original substrate had led to a lower K_{SV} value.

The results obtained in this work are not easy to compare with the literature since different quenching methodologies are frequently used, and the effects of the quencher may be different depending on the origin of the protein hydrolysate. Ma et al. (Ma et al., 2018) obtained K_{SV} values in the range 100–700 M^{-1} for ANS-binding of protein isolates of cottonseed meal, indicating a much higher surface hydrophobicity than the FDHs obtained in this work although deviations could be in part attributed to the different methodology. On the other hand, He et al. (He et al., 2014) obtained K_{SV} values of the same order for peanut protein isolates quenched by ANS-binding. Since quenching rate can be also influenced by the presence of free amino acids with fluorescence emission, an additional quenching experiment was performed with a synthetic solution of free amino acids, which was obtained by mixing commercially available (Sigma Aldrich) standards in ultrapure water according to the free amino acid profile of the WSP hydrolysate obtained by SWH (Table S1). From this experiment, a higher but rather similar K_{SV} value was obtained compared to those of FM and NSP. This result suggests that fluorescence emission of FDHs obtained by SWH is not only due to surface hydrophobicity but also to the release of free amino acids and small peptides during SWH, which present high fluorescent intensities but at the same time high sensitivity to changes in the solvent environment.

3.8. Droplet size measurements

The droplet size distribution of fresh and stored emulsions was used to evaluate the emulsifying ability of FDHs and physical stability of the emulsions during storage for 14 days, as shown in Fig. 5. The droplet diameter, expressed as a volume weighted mean (D[4,3]) can be also used to monitor the evolution of the emulsions along storage and is reported in Table S3.

Fresh emulsions were obtained after 7 passes through the microfluidizer, monitoring the D[4,3] parameter after each pass and observing the droplet size reduction. Droplet size reduction was much more significant in the FM and NSP samples obtained by SWH with reductions from 12 to 14 μm of the coarse emulsion to 0.15–0.2 μm of the final emulsion. Similar results were obtained for pea protein-maltodextrin mixture in the microemulsification of rice bran oil, with a droplet size reduction from 9 μm to 0.2 μm after 8 passes through a microfluidizer (Benito-Román, Sanz, & Beltrán, 2020). On the other hand, WSP samples did not show a significant improvement in D[4,3] and droplet size distribution when increasing the number of passes, whereas the FM and NSP samples treated with Alcalase® suffered a reduction from 40 μm to 7.9 μm and from 12 to 4.6 μm, respectively. Moreover, as it can be seen in Fig. 5, the emulsions obtained with FM and NSP hydrolyzed with Alcalase® (Fig. 5d and f, respectively) presented a larger droplet size than their SWH counterparts (Fig. 5a and c).

As shown in Fig. 5a, emulsions stabilized with FM hydrolysates obtained by SWH exhibited a small droplet size distribution, centered around 0.14 μm just after high-pressure homogenization. This droplet size distribution is similar to those reported by (Lu, Chen, Wang, Yang, & Qi, 2016). for emulsions stabilized by soy protein hydrolysates obtained by SWH, and (Benito-Román et al., 2020) for emulsions stabilized with pea protein and maltodextrin mixtures. However, the emulsions obtained in this work showed lower physical stability, since larger populations (>1.25 μm) started to grow after just 1 day of storage. It has been proposed that protein unfolding and the Maillard reaction products formed during SWH process could decrease the energy barrier for interfacial adsorption during high-speed homogenization (Lu et al., 2016). Moreover, small droplet sizes have been also related to highly hydrolyzed peptides (Lu et al., 2016), although we have observed that the small peptides and amino acids resulting from extensive hydrolysis by SWH process do not contribute to emulsion stability, possibly due to its small size and the inability to form stable surface interactions. On the other hand, the larger peptides obtained from FM treated with Alcalase® (Fig. 5d), which presented a much larger droplet size distribution centered at 7.6 μm, were more stable under storage for 14 days. These larger peptides are more likely to present both hydrophobic and hydrophilic domains, which allow for a more effective and stable interfacial adsorption.

From Fig. 5b and e, we can see that the WSP hydrolysates did not promote the formation of stable emulsions, no matter the hydrolysis method. As shown in the previous analysis, the higher solubility and the low surface hydrophobicity of these hydrolysates possibly prevented surface adsorption and the formation of the strong hydrophobic interactions that are necessary to form a stable emulsion.

The NSP hydrolysates obtained by SWH (Fig. 5c) and Alcalase hydrolysis (Fig. 5f) presented molecular size distributions similar to their FM counterparts, although some improvements in emulsifying properties can be observed. The SWH hydrolysates of NSP allowed the formation of an emulsion with smaller droplet size distribution, compared to FM, that still retains its characteristics after 7 days of storage (Fig. 5c). Moreover, the emulsion obtained using the Alcalase® hydrolysate from NSP maintained the same droplet size for 14 days of storage. These results suggest better emulsifying properties of NSP hydrolysates, possibly related to the higher surface hydrophobicity, the intermediate peptide size and the higher degree of hydrolysis achieved through enzymatic treatment, which leads to a remarkable improvement of physical stability and could be ascribed to the thicker architecture derived from interfacial adsorption of protein fragments and small peptides. Similar findings have been reported by other authors, who proposed that the

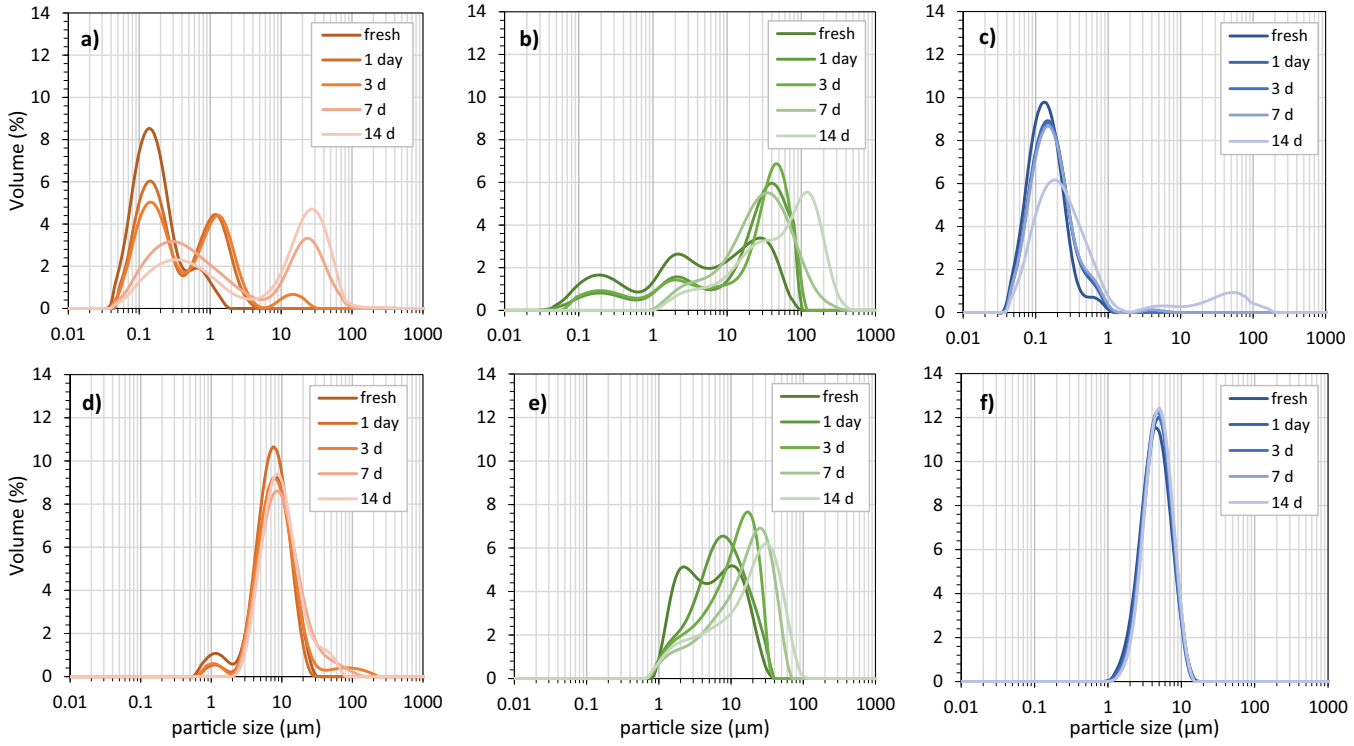

Fig. 5. Droplet size distributions of emulsions stabilized with 2% freeze-dried hydrolysate (FDH) from fish meal (FM, orange), its water-soluble fraction (WSP, green), and its non-water-soluble fraction (NSP, blue) obtained by a,b,c) SWH treatment, d,e,f) Alcalase® hydrolysis. (For interpretation of the references to colour in this figure legend, the reader is referred to the web version of this article.)

formation of a gel-like network of adsorbed protein at the interface could provide a steric hindrance to oil droplets against coalescence (Lu et al., 2016; N. N. Wu et al., 2014; Zhang et al., 2015).

3.9. Electrokinetic potential of emulsion droplets

The electrokinetic potential (i.e. ζ potential) of emulsion droplets stabilized with different FDHs is shown in Fig. S1. The ζ potential of all samples was negative, indicating a predominance of negative charges over positive charges on the surface of the emulsion droplets. It has been generally accepted that the ζ potential of an emulsion is an indicative of its physical stability (Shanmugam & Ashokkumar, 2014). The higher the ζ potential absolute value, the more physically stable is the emulsion because the repulsive forces between electrostatic charges with the same sign prevent the emulsion droplets to aggregate and collapse, resulting in a physically stable system.

For the emulsions obtained in this work, the ζ potential follows different patterns that can be related to its physical stability, as observed in the measurement of droplet size distribution. The emulsions formulated with WSP hydrolysates presented low initial values for the ζ potential (around −10 mV), which suggest less repulsive interactions and poor physical stability due to the tendency of the emulsion droplets to aggregate. For these emulsions, the zeta potential also increases and gets closer to zero when increasing storage time, indicating that destabilization is occurring due to the neutralization of positive and negative charges on the droplet surface caused by flocculation. This extreme has been confirmed by adding a deflocculant (SDS) to the emulsion prior to the measurement of droplet size distribution and zeta potential, as described by (Santos, Calero, Muñoz, & Cidade, 2018). According to the data presented in Table 6, D[4,3] of the emulsions after 14 days of storage at 4 °C was reduced with the addition of SDS in all cases, with percentual decreases ranging from 14 to 95%. These results indicate that the increase in the average droplet size during storage was mainly due to flocculation, instead of coalescence. Comparable results were obtained by (Benito-Román et al., 2020) for microemulsions of rice bran oil stabilized with pea protein and maltodextrin mixtures.

The emulsions formulated with FM and NSP showed higher (in absolute value) zeta potential values, ranging from −18.5 to −27.3 mV. It has been suggested that the emulsions with zeta potential values of −11 to −20 mV were close to the threshold of destabilization, while the emulsions with higher absolute values of zeta potential (−41 to −50 mV) had good stability (Shanmugam & Ashokkumar, 2014). From the data presented in Fig. 5 and the evolution of the droplet size distribution of the hydrolysates, the emulsions obtained with NSP hydrolysates are stable no matter the hydrolysis method. On the contrary, the emulsions formulated with FM presented differences with the hydrolysis method. The SWH hydrolysate led to an emulsion with higher zeta potential (−23.5 mV) than the one obtained with the enzymatic FM hydrolysate (−18.5 mV). However, the first emulsion rapidly crossed the destabilization threshold, showing a zeta potential of −11.5 mV after 1 day of storage, whereas the latter kept its physical stability and its zeta potential value along 14 days of storage. Again, the larger peptides produced by Alcalase®, compared to the smaller protein fragments and free amino acids obtained by SWH treatment offer an explanation to these results. The smaller the size of the peptides, the more likely to adsorb on the droplet surface, conferring its electrical charge (i.e.: higher zeta potential); however, an excessively small size of peptides and amino acids does not allow the formation of a thick protein layer around the oil droplet and the emulsion ultimately collapses. On the contrary, the larger peptides obtained with Alcalase® do not provide a high surface charge but they could act as Pickering-like stabilizers, giving strong emulsion architectures derived from interfacial adsorption of protein aggregates in thick layers, and effectively improving the creaming stability of emulsion (N. Li et al., 2022; Liu & Tang, 2013). Zeta potential results are also closely related to surface hydrophobicity since when the absolute value of zeta potential of protein solution becomes smaller and electrostatic repulsion is reduced, the protein molecules in the system tend to aggregate with each other. As a result, the hydrophobic groups of the protein become embedded in the protein aggregates; thus, reducing the surface hydrophobicity of the protein residues and decreasing emulsion stability (D. Li et al., 2020).

4. Conclusions

Subcritical water hydrolysis (SWH) raises as a green and efficient method to prepare fish protein hydrolysates from fish meal (FM), its water-soluble fraction (WSP) and insoluble fraction (NSP). Compared to enzymatic hydrolysis, SWH provides higher hydrolysis yield, higher protein recovery, and higher degree of hydrolysis, no matter the starting material. The techno-functional properties of fish protein hydrolysates explored in this work are highly intercorrelated. i.e., small peptides and amino acids present good solubility in a broad pH range, which opens its utilization in pharmaceutical and cosmeceutical applications. The best emulsifying properties and highest emulsion stability were observed in fish protein hydrolysates with intermediate peptide sizes and high surface hydrophobicity, such as the NSP hydrolysates. This work demonstrates that fish protein hydrolysates can be prepared using water, the greenest solvent, as the extraction solvent and the hydrolytic agent. Furthermore, the prior fractionation by conventional water extraction allowed to obtain hydrolysates with different properties, which can be targeted to specific applications. In this work, the techno-functional properties of the NSP hydrolysates were improved, yielding emulsions with lower droplet sizes and better stability than other green alternatives such as enzymatic hydrolysis. On the other hand, the hydrolyzed WSP fraction did not present good emulsifying properties, although it represents a valuable source of N in the form of free and structural amino acids with numerous industrial applications.

CRediT authorship contribution statement

Pedro Barea: Investigation, Methodology, Writing – review & editing. **Rodrigo Melgosa:** Conceptualization, Data curation, Supervision, Writing – original draft, Writing – review & editing. **Óscar Benito-Román:** Investigation, Supervision, Writing – review & editing. **Alba Esther Illera:** Investigation, Methodology, Writing – review & editing. **Sagrario Beltrán:** Funding acquisition, Project administration, Writing – review & editing. **María Teresa Sanz:** Conceptualization, Funding acquisition, Project administration, Supervision, Writing – review & editing.

Declaration of competing interest

Authors declare no conflict of interest.

Data availability

Data will be made available on request.

Acknowledgments

The authors acknowledge Sarval Bio-Industries Noroeste, S.A.U. (A Coruña, Spain) for kindly providing the fish meal used in this work and Novozymes A/S for kindly providing the enzyme Alcalase®. This work was supported by the Agencia Estatal de Investigación (AEI) [grant numbers PID2019-104950RB-I00 and PID2020-116716RJ-I00] by the AEI, Ministerio de Ciencia e Innovación (MICINN) and Next GenerationEU, [grant numbers TED2021-129311B-I00 and PDC2022-133443-I00] and the Junta de Castilla y León (JCyL) and the European Regional Development Fund (ERDF) [grant number BU050P20]. PB predoctoral contract is funded by JCyL and the European Social Fund (ESF) [ORDEN EDU/1868/2022]. RM contract is funded by a Beatriz Galindo Research Fellowship [BG20/00182]. Illera's post-doctoral contract is

funded by AEI, MICINN and EU through project TED2021-129311B-I00. OBR post-doctoral contract was funded by AEI through project PID2020–116716RJ-I00.

Appendix A. Supplementary data

Supplementary data to this article can be found online at https://doi.org/10.1016/j.foodchem.2024.139550.

References

Abdelmoez, W., Nakahasi, T., & Yoshida, H. (2007). Amino acid transformation and decomposition in saturated subcritical water conditions. *Industrial & Engineering Chemistry Research, 46*, 5286–5294. https://doi.org/10.1021/ie070151b

Adler-Nissen, J. (1979). Determination of the degree of hydrolysis of food protein hydrolysates by trinitrobenzenesulfonic acid. *Journal of Agricultural and Food Chemistry, 27*, 1256–1262. https://doi.org/10.1021/jf60226a042

Ali, M. S., Ho, T. C., Razack, S. A., Haq, M., Roy, V. C., Park, J. S., … Chun, B. S. (2023). Oligochitosan recovered from shrimp shells through subcritical water hydrolysis: Molecular size reduction and biological activities. *Journal of Supercritical Fluids, 196*. https://doi.org/10.1016/j.supflu.2023.105868

Antonov, Y. A., Zhuravleva, I. L., Cardinaels, R., & Moldenaers, P. (2015). Structural studies on the interaction of lysozyme with dextran sulfate. *Food Hydrocolloids, 44*, 71–80. https://doi.org/10.1016/j.foodhyd.2014.09.006

Arogundade, L. A., Mu, T. H., & Akinhanmi, T. F. (2016). Structural, physicochemical and interfacial stabilisation properties of ultrafiltered African yam bean (*Sphenostylis stenocarpa*) protein isolate compared with those of isoelectric protein isolate. *LWT - Food Science and Technology, 69*, 400–408. https://doi.org/10.1016/j.lwt.2016.01.049

Aspevik, T., Egede-Nissen, H., & Oterhals, Å. (2016). A systematic approach to the comparison of cost efficiency of endopeptidases for the hydrolysis of Atlantic salmon (*Salmo salar*) by-products. *Food Technology and Biotechnology, 54*(4), 421–431. https://doi.org/10.17113/ft b.54.04.16.4553

Barea, P., Melgosa, R., Illera, A. E., Alonso-Riaño, P., Díaz de Cerio, E., Benito-Román, O., … Teresa Sanz, M. (2023). Production of small peptides and low molecular weight amino acids by subcritical water from fish meal: Effect of pressurization agent. *Food Chemistry, 418*, Article 135925. https://doi.org/10.1016/j.foodchem.2023.135925

Benito-Román, Ó., Sanz, M. T., Illera, A. E., Melgosa, R., Benito, J. M., & Beltrán, S. (2019). Pectin methylesterase inactivation by high pressure carbon dioxide (HPCD). *Journal of Supercritical Fluids, 145*. https://doi.org/10.1016/j.supflu.2018.11.009

Benito-Román, Sanz, T., & Beltrán, S. (2020). Microencapsulation of rice bran oil using pea protein and maltodextrin mixtures as wall material. *Heliyon, 6*, Article e03615. https://doi.org/10.1016/j.heliyon.2020.e03615

Bobone, S., Van De Weert, M., & Stella, L. (2014). A reassessment of synchronous fluorescence in the separation of Trp and Tyr contributions in protein emission and in the determination of conformational changes. *Journal of Molecular Structure, 1077*, 68–76. https://doi.org/10.1016/j.molstruc.2014.01.004

Boisen, S., Bech-Andersen, S., & Eggum, B. O. (1987). A critical view on the conversion factor 6.25 from total nitrogen to protein. *Acta Agriculturae Scandinavica, 37*, 299–304. https://doi.org/10.1080/00015128709436560

Brishti, F. H., Chay, S. Y., Muhammad, K., Ismail-Fitry, M. R., Zarei, M., Karthikeyan, S., & Saari, N. (2020). Effects of drying techniques on the physicochemical, functional, thermal, structural and rheological properties of mung bean (*Vigna radiata*) protein isolate powder. *Food Research International, 138 Part B*, Article 109783. https://doi.org/10.1016/j.foodres.2020.109783

Chen, Y., Chen, J., Chang, C., Chen, J., Cao, F., Zhao, J., Zheng, Y., & Zhu, J. (2019). Physicochemical and functional properties of proteins extracted from three microalgal species. *Food Hydrocolloids, 96*, 510–517. https://doi.org/10.1016/j.foodhyd.2019.05.025

Chun, B. S., Lee, S. C., Ho, T. C., Micomyiza, J. B., Park, J. S., & Lee, H. J. (2022). Subcritical water hydrolysis of comb pen shell (*Atrina pectinata*) edible parts to produce high-value amino acid products. *Marine Drugs, 20*(6). https://doi.org/10.3390/md20060357

Das, D., Mir, N. A., Chandla, N. K., & Singh, S. (2021). Combined effect of pH treatment and the extraction pH on the physicochemical, functional and rheological characteristics of amaranth (*Amaranthus hypochondriacus*) seed protein isolates. *Food Chemistry, 353*, Article 129466. https://doi.org/10.1016/j.foodchem.2021.129466

Diniz, G. S., Barbarino, E., Oiano-Neto, J., Pacheco, S., & Lourenço, S. O. (2013). Gross chemical profile and calculation of nitrogen-to-protein conversion factors for nine species of fishes from coastal waters of Brazil. *Latin American Journal of Aquatic Research, 41*, 254–264. https://doi.org/10.3856/vol41-issue2-fulltext-5

FAO. (2022). *The state of world fisheries and aquaculture 2022*. Towards Blue Transformation: Rome, FAO. https://doi.org/10.4060/cc0461en

Friedman, M. (2004). Applications of the ninhydrin reaction for analysis of amino acids, peptides, and proteins to agricultural and biomedical sciences. *Journal of Agricultural and Food Chemistry, 52*, 385–406. https://doi.org/10.1021/jf030490p

Gehring, C., Davenport, M., & Jaczynski, J. (2009). Functional and nutritional quality of protein and lipid recovered from fish processing by-products and underutilized aquatic species using isoelectric solubilization/precipitation. *Current Nutrition & Food Science, 5*, 17–39. https://doi.org/10.2174/157340109787314703

He, X. H., Liu, H. Z., Liu, L., Zhao, G. L., Wang, Q., & Chen, Q. L. (2014). Effects of high pressure on the physicochemical and functional properties of peanut protein isolates. *Food Hydrocolloids, 36*, 123–129. https://doi.org/10.1016/j.foodhyd.2013.08.031

Li, C., Xue, H., Chen, Z., Ding, Q., & Wang, X. (2014). Comparative studies on the physicochemical properties of peanut protein isolate-polysaccharide conjugates prepared by ultrasonic treatment or classical heating. *Food Research International, 57*, 1–7. https://doi.org/10.1016/j.foodres.2013.12.038

Li, D., Zhao, Y., Wang, X., Tang, H., Wu, N., Wu, F., Yu, D., & Elfalleh, W. (2020). Effects of (+)-catechin on a rice bran protein oil-in-water emulsion: Droplet size, zeta-potential, emulsifying properties, and rheological behavior. *Food Hydrocolloids, 98*, Article 105306. https://doi.org/10.1016/j.foodhyd.2019.105306

Li, N., Wang, Y., Gan, Y., Wang, S., Wang, Z., Zhang, C., & Wang, Z. (2022). Physicochemical and functional properties of protein isolate recovered from *Rana chensinensis* ovum based on different drying techniques. *Food Chemistry, 396*, Article 133632. https://doi.org/10.1016/j.foodchem.2022.133632

Liu, F., & Tang, C. H. (2013). Soy protein nanoparticle aggregates as Pickering stabilizers for oil-in-water emulsions. *Journal of Agricultural and Food Chemistry, 61*, 8888–8898. https://doi.org/10.1021/jf401859y

López, D. N., Boeris, V., Spelzini, D., Bonifacino, C., Panizzolo, L. A., & Abirached, C. (2019). Adsorption of chia proteins at interfaces: Kinetics of foam and emulsion formation and destabilization. *Colloids and Surfaces B: Biointerfaces, 180*, 503–507. https://doi.org/10.1016/j.colsurfb.2019.04.067

Lu, W., Chen, X. W., Wang, J. M., Yang, X. Q., & Qi, J. R. (2016). Enzyme-assisted subcritical water extraction and characterization of soy protein from heat-denatured meal. *Journal of Food Engineering, 169*, 250–258. https://doi.org/10.1016/j.jfoodeng.2015.09.006

Lv, Y., Chen, L., Liu, F., Xu, F., & Zhong, F. (2023). Improvement of the encapsulation capacity and emulsifying properties of soy protein isolate through controlled enzymatic hydrolysis. *Food Hydrocolloids, 138*, Article 108444. https://doi.org/10.1016/j.foodhyd.2022.108444

Ma, M., Ren, Y., Xie, W., Zhou, D., Tang, S., Kuang, M., Wang, Y., Du, S., & kui.. (2018). Physicochemical and functional properties of protein isolate obtained from cottonseed meal. *Food Chemistry, 240*, 856–862. https://doi.org/10.1016/j.foodchem.2017.08.030

Marcet, I., Álvarez, C., Paredes, B., & Díaz, M. (2016). The use of sub-critical water hydrolysis for the recovery of peptides and free amino acids from food processing wastes. Review of sources and main parameters. *Waste Management, 49*, 364–371. https://doi.org/10.1016/j.wasman.2016.01.009

Melgosa, R., Marques, M., Paiva, A., Bernardo, A., Fernández, N., Sá-Nogueira, I., & Simões, P. (2021). Subcritical water extraction and hydrolysis of cod (*Gadus morhua*) frames to produce bioactive protein extracts. *Foods, 10*(6). https://doi.org/10.3390/foods10061222

Melgosa, R., Trigueros, E., Sanz, M. T., Cardeira, M., Rodrigues, L., Fernández, N., … Simões, P. (2020). Supercritical CO_2 and subcritical water technologies for the production of bioactive extracts from sardine (*Sardina pilchardus*) waste. *Journal of Supercritical Fluids, 164*. https://doi.org/10.1016/j.supflu.2020.104943

O'Sullivan, J., Beevers, J., Park, M., Greenwood, R., & Norton, I. (2015). Comparative assessment of the effect of ultrasound treatment on protein functionality pre- and post-emulsification. *Colloids and Surfaces A: Physicochemical and Engineering Aspects, 484*, 89–98. https://doi.org/10.1016/j.colsurfa.2015.07.065

Paiva dos Santos, K., Mellinger-Silva, C., Santa Brígida, A. I., & Barros Gonçalves, L. R. (2020). Modifying alcalase activity and stability by immobilization onto chitosan aiming at the production of bioactive peptides by hydrolysis of tilapia skin gelatin. *Process Biochemistry, 97*, 27–36. https://doi.org/10.1016/j.procbio.2020.06.019

Park, J. S., Roy, V. C., Kim, S. Y., Lee, S. C., & Chun, B. S. (2022). Extraction of edible oils and amino acids from eel by-products using clean compressed solvents: An approach of complete valorization. *Food Chemistry, 388*(April), Article 132949. https://doi.org/10.1016/j.foodchem.2022.132949

Rivas-Ubach, A., Liu, Y., Bianchi, T. S., Tolić, N., Jansson, C., & Paša-Tolić, L. (2018). Moving beyond the van Krevelen diagram: A new stoichiometric approach for compound classification in organisms. *Analytical Chemistry, 90*(10), 6152–6160. https://doi.org/10.1021/acs.analchem.8b00529

Salo-Väänänen, P. P., & Koivistoinen, P. E. (1996). Determination of protein in foods: Comparison of net protein and crude protein (N x 6.25) values. *Food Chemistry, 57*, 27–31. https://doi.org/10.1016/0308-8146(96)00157-4

Santos, J., Calero, N., Muñoz, J., & Cidade, M. T. (2018). Development of food emulsions containing an advanced performance xanthan gum by microfluidization technique. *Food Science and Technology International, 24*, 373–381. https://doi.org/10.1177/1082013218756140

Shahidi, F., Varatharajan, V., Peng, H., & Senadheera, R. (2019). Utilization of marine by-products for the recovery of value-added products. *Journal of Food Bioactives, 6*, 10–61. https://doi.org/10.31665/jfb.2019.6184

Shanmugam, A., & Ashokkumar, M. (2014). Ultrasonic preparation of stable flax seed oil emulsions in dairy systems - physicochemical characterization. *Food Hydrocolloids, 39*, 151–162. https://doi.org/10.1016/j.foodhyd.2014.01.006

Sluiter, J. B., Ruiz, R. O., Scarlata, C. J., Sluiter, A. D., & Templeton, D. W. (2010). Compositional analysis of lignocellulosic feedstocks. 1. Review and description of methods. *Journal of Agricultural and Food Chemistry, 58*, 9043–9053. https://doi.org/10.1021/jf1008023

Trigueros, E., Sanz, M. T., Alonso-Riaño, P., Beltrán, S., Ramos, C., & Melgosa, R. (2021). Recovery of the protein fraction with high antioxidant activity from red seaweed industrial solid residue after agar extraction by subcritical water treatment. *Journal of Applied Phycology, 33*, 1181–1194. https://doi.org/10.1007/s10811-020-02349-0

Wisuthiphaet, N., & Kongruang, S. (2015). Production of fish protein hydrolysates by acid and enzymatic hydrolysis. *Journal of Medical and Bioengineering, 4*, 466–470. https://doi.org/10.12720/jomb.4.6.466-470

Wu, H., Forghani, B., Abdollahi, M., & Undeland, I. (2022). Lipid oxidation in sorted herring (*Clupea harengus*) filleting co-products from two seasons and its relationship

to composition. *Food Chemistry, 373*, Article 131523. https://doi.org/10.1016/j.foodchem.2021.131523

Wu, N. N., Zhang, J. B., Tan, B., He, X. T., Yang, J., Guo, J., & Yang, X. Q. (2014). Characterization and interfacial behavior of nanoparticles prepared from amphiphilic hydrolysates of β-conglycinin-dextran conjugates. *Journal of Agricultural and Food Chemistry, 62*, 12678–12685. https://doi.org/10.1021/jf504173z

Zhang, Q. T., Tu, Z. C., Wang, H., Huang, X. Q., Fan, L. L., Bao, Z. Y., & Xiao, H. (2015). Functional properties and structure changes of soybean protein isolate after subcritical water treatment. *Journal of Food Science and Technology, 52*, 3412–3421. https://doi.org/10.1007/s13197-014-1392-9